Revision 4

Supplementary materials for sound velocities across calcite phase transitions by Brillouin scattering spectroscopy

Chao-shuai Zhao[1,2], He-ping Li[1*], Po-fei Chen[3], Jian-jun Jiang[1]

[1]*Key Laboratory of High-temperature and High-pressure Study of the Earth's Interior, Institute of Geochemistry, Chinese Academy of Sciences, 550081 Guiyang, China*

[2] *College of Earth Sciences, University of Chinese Academy of Sciences, 100049 Beijing, China*

[3]*Department of Earth Sciences, National Central University, 32001 Taoyuan, Taiwan, China*

*Corresponding author. Email: liheping@vip.gyig.ac.cn

Supplemental Table S1. Previous studies of the elastic constants of calcite at ambient conditions.

C_{11} (GPa)	C_{33} (GPa)	C_{44} (GPa)	C_{12} (GPa)	C_{13} (GPa)	C_{14} (GPa)	K_{VRH} (GPa)	G_{VRH} (GPa)
144.5±1.0[a]	83.1±0.5	32.7±0.3	57.1±1.0	53.4±2.0	20.5±0.6		
146.3±0.7[b]	85.3±0.5	34.0±0.2	59.7±1.1	50.8±3.3	20.8±0.6	74.7	31.8
148.0±0.2[b]	85.7±0.1	32.7±0.1	55.4±0.9	54.5±2.4	20.8±0.6	76.1	31.8
145.7[c]	85.3	33.4	55.9	53.5	20.5	75.3	31.7
140.9[d]	85.8	33.4	63.7	62.6	19.5		
149.7±0.7[e]	85.2±1.8	34.1±0.5	57.9±1.1	53.5±0.9	20.0±0.2	76.1	32.8
146.82[f]	91.76	32.52	47.87	46.05	16.81		
149.9±0.5[g]	87.0±0.4	32.2±0.2	59.5±0.2	57.3±0.3	17.9±0.2	78.6±0.4	32.1±0.2
177[h]	95	39	78	72	25	97	40

VRH represents Voigt-Reuss-Hill average;
a: Pulse-echo method, Peselnick and Robie 1963;
b: Pulse-echo method and phase-comparison method, Dandekar 1968;
c: Pulse-echo-overlap method, Thanh and Lacam 1984;
d: Theoretical calculation, Fisler et al. 2000;
e: Brillouin scattering, Chen et al. 2001;
f: Density functional theory, Zhao et al. 2009;
g: Brillouin scattering, Lin 2013;
h: Density functional theory, Marcondes et al. 2016.

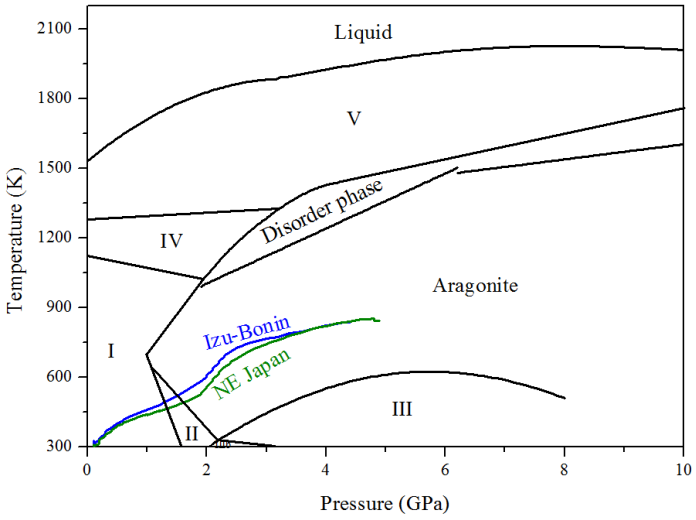

Supplemental Figure S1. Phase diagram of $CaCO_3$. Phase boundary lines as follows. I-II: (Liu et al. 2017); II-III: (Bayarjargal et al. 2018; Suito et al. 2001; Liu et al. 2017; Pippinger et al. 2015); II-IIIb: (Pippinger et al. 2015; Schaebitz et al. 2015); I-Aragonite: (Bayarjargal et al. 2018; Litasov et al. 2017; Ter Heege and Renner 2007); II-Aragonite: (Liu et al. 2017); I-IV: (Bayarjargal et al. 2018; Litasov et al. 2017; Shatskiy et al. 2014; Ter Heege and Renner 2007); III-Aragonite: (Bayarjargal et al. 2018; Suito et al. 2001; Li et al. 2015; Schaebitz et al. 2015); IV-V: (Bayarjargal et al. 2018; Shatskiy et al. 2014; Ter Heege and Renner 2007); IV-disordered phase: (Shatskiy et al. 2014); V-Aragonite: (Bayarjargal et al. 2018; Li et al. 2017; Litasov et al. 2017; Shatskiy et al. 2014; Ter Heege and Renner 2007); Aragonite-disordered phase: (Suito et al. 2001); Disordered phase-Aragonite: (Litasov et al. 2017); V-Liquid: (Bayarjargal et al. 2018; Li et al. 2017; Shatskiy et al. 2014). The modeled subduction zone temperature and pressure lines for the NE Japan and Izu-Bonin regions are from Peacock (2003). Blue line: Izu-Bonin; olive line: NE Japan.

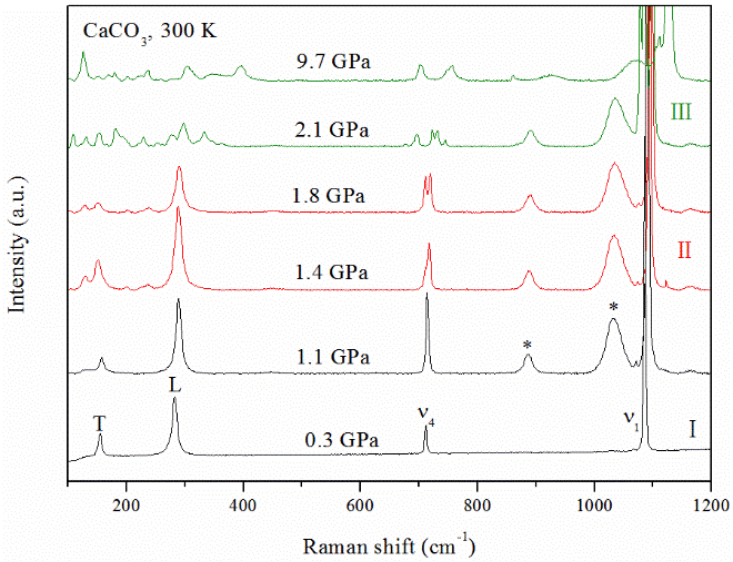

Supplemental Figure S2. Representative Raman spectra of $CaCO_3$ as a function of pressure at ambient temperature. Stars represent the signal of methanol and ethanol mixture.

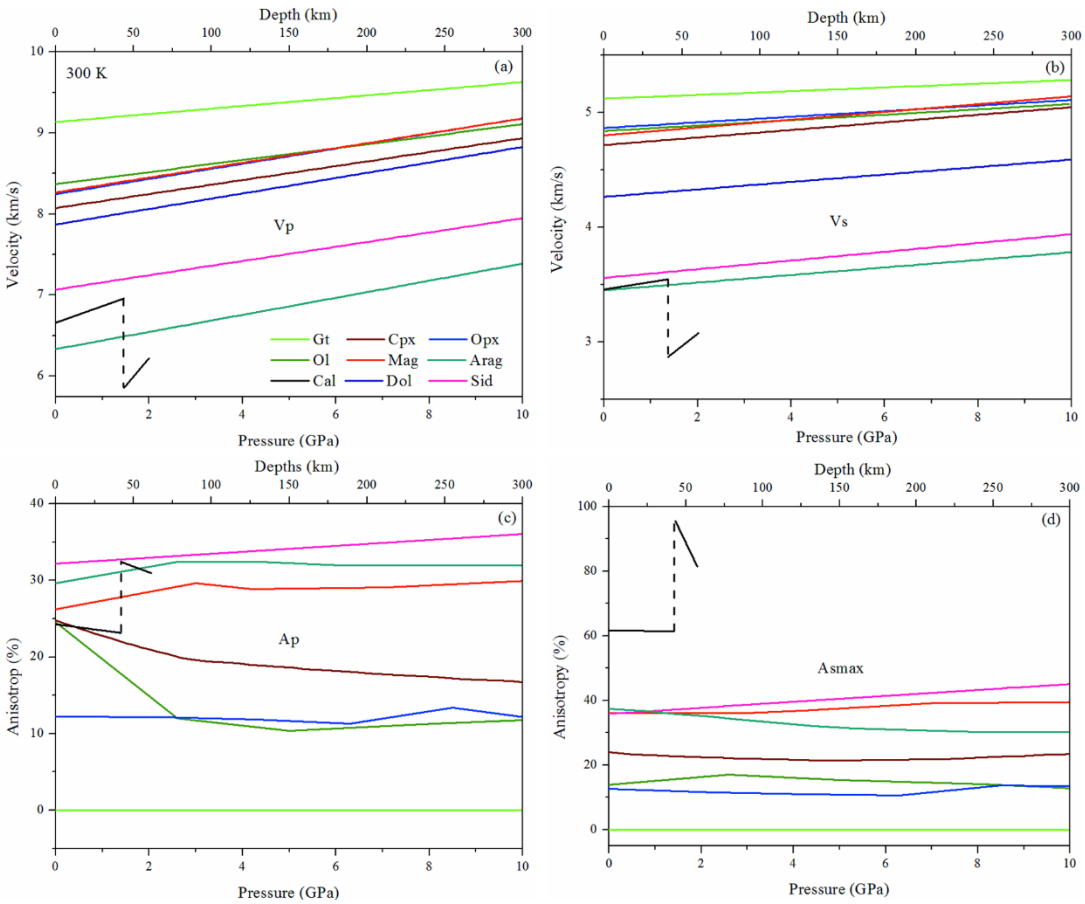

Figure S3. Pressure dependence of Vp (a) and Vs (b) velocities and Ap (c) and Asmax (d) anisotropies of carbonates and major upper mantle minerals at 300 K.

Black lines: calcite (Cal) (this study; Chen et al. 2001); dark cyan lines: aragonite (Arag) (Huang et al. 2017; Liu et al. 2005; Marcondes et al. 2016); olive lines: olivine (Ol) (Mao et al. 2015; Zha et al. 1998); green lines: garnet (Gt) (Lu et al. 2013; Sinogeikin and Bass 2000); wine lines: clinopyroxene (Cpx) (Duffy and Anderson 1989; Sang and Bass 2014; Collins and Brown 1998; Zou et al. 2018); blues lines: orthopyroxene (Opx) (Chai et al. 1997; Duffy and Anderson 1989); red lines: magnesite (Mag) (Yang et al. 2014; Sanchez-Valle et al. 2011); navy lines: dolomite (Dol) (Marcondes et al. 2016); pink lines: siderite (Sid) (Sanchez-Valle et al. 2011; Stekiel et al. 2017).

References cited

Bayarjargal, L., Fruhner, C.-J., Schrodt, N., and Winkler, B. (2018) $CaCO_3$ phase diagram studied with Raman spectroscopy at pressures up to 50 GPa and high-temperatures and DFT modeling. Physics of the Earth and Planetary Interiors, 281, 31–45.

Chai, M., Brown, J.M., and Slutsky, L.J. (1997) The elastic constants of an aluminous orthopyroxene to 12.5 GPa. Journal of Geophysical Research, 102, 14779–14785.

Chen, C.-C., Lin, C.-C., Liu, L.-G., Sinogeikin, S.V. and Bass, J.D. (2001) Elasticity of single-crystal calcite and rhodochrosite by Brillouin spectroscopy. American Mineralogist, 86, 1525–1529.

Collins, M.D., and Brown, J.M. (1998) Elasticity of an upper mantle clinopyroxene. Physics and Chemistry of Minerals, 26, 7-13.

Dandekar, D.P. (1968) Elastic constants of calcite. Journal of Applied Physics, 39(6), 2971-2973.

Duffy, T.S., and Anderson, D.L. (1989) Seismic velocities in mantle minerals and the mineralogy of the upper mantle. Journal of Geophysical Research, 94(B2), 1895-1912.

Fisler, D.K., Gale, J.D., and Cygan, R.T. (2000) A shell model for the simulation of rhombohedral carbonate minerals and their point defects. American Mineralogist, 85, 217-224.

Huang, D., Liu, H., Hou, M.-Q., Xie, M.-Y., Lu, Y.-F., Liu, L., Yi, L., Cui, Y.-J., Li, Y., Deng, L.-W., and Du, J.-G. (2017) Elastic properties of $CaCO_3$ high-pressure phases from first principles. Chinese Physics B, 26, 089101.

Li, Y., Zou, Y., Chen, T., Wang, X., Qi, X., Chen, H., Du, J., and Li, B. (2015) P-V-T

equation of state and high-pressure behavior of $CaCO_3$ aragonite. American Mineralogist, 100, 2323-2329.

Li, Z., Li, J., Lange, R., Liu, J., and Militzer, B. (2017) Determination of calcium carbonate and sodium carbonate melting curves up to Earth's transition zone pressures with implications for the deep carbon cycle. Earth and Planetary Science Letters, 457, 395-402.

Lin, C.-C. (2013) Elasticity of calcite: thermal evolution. Physics and Chemistry of Minerals, 40, 157–166.

Litasov, K.D., Shatskiy, A., Gavryushkin, P.N., Bekhtenova, A.E., Dorogokupets, P.I., Danilov, B.S., Higo, Y., Akilbekov, A.T., and Inerbaev, T.M. (2017) P-V-T equation of state of $CaCO_3$ aragonite to 29 GPa and 1673 K: In situ X-ray diffraction study. Physics of the Earth and Planetary Interiors, 265, 82-91.

Liu, C.-J, Zheng, H.-F, and Wang, D.-J. (2017) Raman spectroscopic study of calcite III to aragonite transformation under high-pressure and high-temperature. High Pressure Research, 37(4), 545-557.

Liu, L.-G., Chen, C.-C., Lin, C.-C., and Yang, Y.-J. (2005) Elasticity of single-crystal aragonite by Brillouin spectroscopy. Physics and Chemistry of Minerals, 32, 97-102.

Lu, C., Mao, Z., Lin, J.-F., Zhuravlev, K.K., Tkachev, S.N., and Prakapenka, V.B. (2013) Elasticity of single-crystal iron-bearing pyrope up to 20 GPa and 750 K. Earth and Planetary Science Letters, 361, 134–142.

Mao, Z., Fan, D.-W., Lin, J.-F., Yang, J., Tkachev, S.N., Zhuravlev, K., and Prakapenka, V.B. (2015) Elasticity of single-crystal olivine at high-pressures and temperatures. Earth and Planetary Science Letters, 426, 204-215.

Marcondes, M.L., Justo, J.F., and Assali, L.V.C. (2016) Carbonates at high-pressures:

Possible carriers for deep carbon reservoirs in the Earth's lower mantle. Physical Review B, 94, 104112.

Peacock, S.M. (2003) Thermal structure and metamorphic evolution of subducting slabs. In J.M. Eiler Eds., Inside the Subduction Factory, Geophysical Monograph, p. 7–22. AGU Press, Washington, D.C.

Peselnick, L., and Robie, R.A. (1963) Elastic constants of calcite. Journal of Applied Physics, 34(8), 2494-2495.

Pippinger, T., Miletich, R., Merlini, M., Lotti, P., Schouwink, P., Yagi, T., Crichton, W.A., and Hanfland, M. (2015) Puzzling calcite-III dimorphism: crystallography, high-pressure behavior, and pathway of single-crystal transitions. Physics and Chemistry of Minerals, 42, 29–43.

Sanchez-Valle, C., Ghosh, S., and Rosa, A.D. (2011) Sound velocities of ferromagsian carbonates and the seismic detection of carbonates in eclogites and the mantle. Geophysical Research Letters, 38, L24315.

Sang, L.-Q., and Bass, J.D. (2014) Single-crystal elasticity of diopside to 14 GPa by Brillouin scattering. Physics of the Earth and Planetary Interiors, 228, 75–79.

Schaebitz, M., Wirth, R., Janssen, C., and Dresen, G. (2015) First evidence of $CaCO_3$-III and $CaCO_3$-IIIb high-pressure polymorphs of calcite: Authigenically formed in near surface sediments. American Mineralogist, 100(5-6), 1230-1235.

Shatskiy, A., Borzdov, Y.M., Litasov, K.D., Kupriyanov, I.N., Ohtani, E., and Palyanov, Y.N. (2014) Phase relations in the system $FeCO_3$-$CaCO_3$ at 6 GPa and 900-1700 °C and its relation to the system $CaCO_3$-$FeCO_3$-$MgCO_3$. American Mineralogist, 99(4), 773-785.

Sinogeikin, S.V., and Bass, J.D. (2000) Single-crystal elasticity of pyrope and MgO to

20 GPa by Brillouin scattering in the diamond cell. Physics of the Earth and Planetary Interiors, 120, 43-62.

Stekiel, M., Nguyen-Thanh, T., Chariton, S., McCammon, C., Bosak, A., Morgenroth, W., Milman, V., Refson, K., and Winkler, B. (2017) High-pressure elasticity of $FeCO_3$-$MgCO_3$ carbonates. Physics of the Earth and Planetary Interiors, 271, 57–63.

Suito, K., Namba, J., Horikawa, T., Taniguchi, Y., Sakurai, N., Kobayashi, M., Onodera, A., Shimomura, O., and Kikegawa, T. (2001) Phase relations of $CaCO_3$ at high-pressure and high-temperature. American Mineralogist, 86, 997–1002.

Ter Heege, J.H., and Renner, J. (2007) In situ impedance spectroscopy on pyrophyllite and $CaCO_3$ at high-pressure and temperature: phase transformations and kinetics of atomistic transport. Physics and Chemistry of Minerals, 34(7), 445-465.

Thanh, D.V., and Lacam, A. (1984) Experimental study of the elasticity of single crystalline calcite under high-pressure (the calcite I-calcite II transition at 14.6 kbar). Physics of the Earth and Planetary Interiors, 34, 195–203.

Yang, J., Mao, Z., Lin, J.-F., and Prakapenka, V.B. (2014) Single-crystal elasticity of the deep-mantle magnesite at high-pressure and temperature. Earth and Planetary Science Letters, 392, 292–299.

Zha, C.-S., Duffy, T.S., and Downsc, R.T. (1998) Brillouin scattering and X-ray diffraction of San Carlos olivine direct pressure determination to 32 GPa. Earth and Planetary Science Letters, 159, 25-33.

Zhao, J., Zhou, B., Liu, B., and Guo, W. (2009) Elasticity of single-crystal calcite by first-principles calculations. Journal of Computational and Theoretical

Nanoscience, 6, 1181–1188.

Zou, F., Wu, Z.-Q., Wang, W.-Z., Wentzcovitch, R.M. (2018) An extended semianalytical approach for thermoelasticity of monoclinic crystals: application to diopside. Journal of Geophysical Research: Solid Earth, 10.1029/2018JB016-102.